Proc. Natl. Acad. Sci. USA
Vol. 92, pp. 7292–7296, August 1995
Chemistry

Ultrafast thermally induced unfolding of RNase A

C. M. PHILLIPS, Y. MIZUTANI, and R. M. HOCHSTRASSER

Department of Chemistry, University of Pennsylvania, Philadelphia, PA 19104

Contributed by R. M. Hochstrasser, March 9, 1995

ABSTRACT **A temperature jump (T-jump) method capable of initiating thermally induced processes on the picosecond time scale in aqueous solutions is introduced. Protein solutions are heated by energy from a laser pulse that is absorbed by homogeneously dispersed molecules of the dye crystal violet. These act as transducers by releasing the energy as heat to cause a T-jump of up to 10 K with a time resolution of 70 ps. The method was applied to the unfolding of RNase A. At pH 5.7 and 59°C, a T-jump of 3–6 K induced unfolding which was detected by picosecond transient infrared spectroscopy of the amide I region between 1600 and 1700 cm^{-1}. The difference spectral profile at 3.5 ns closely resembled that found for the equilibrium (native − unfolded) states. The signal at 1633 cm^{-1}, corresponding to the β-sheet structure, achieved 15 ± 2% of the decrease found at equilibrium, within 5.5 ns. However, no decrease in absorbance was detected until 1 ns after the T-jump. The disruption of β-sheet therefore appears to be subject to a delay of ≈1 ns. Prior to 1 ns after the T-jump, water might be accessing the intact hydrophobic regions.**

Questions concerning the physical and chemical nature of protein folding are among the most challenging in biological research (1–4). Folding and unfolding events have seldom been studied on time scales shorter than milliseconds. Internal motions of macromolecules such as rotations about single bonds, chemical exchange reactions, diffusion over molecular dimensions, and barrier crossing processes can occur on nanosecond or even picosecond time scales, so protein structure reorganization might be expected to involve ultrafast intermediate steps. An example is the recent report of tens-of-microseconds folding in cytochrome *c* (5). Some of the faster processes in protein folding might involve relatively small alterations in electronic structure. Therefore the probes used to examine them must be sensitive to subtle changes in, for example, nonbonded interactions, weaker chemical bonds, charge distributions, and motions of pieces of the structure. For this reason we decided to use transient infrared (IR) spectroscopy (6–8), which is structure sensitive at a chemical-bond resolution, to identify any ultrafast folding steps.

The IR spectra of proteins in the region of the amide vibrations of the polypeptide structures are well known to be sensitive to the state of the protein. For example, there are distinct differences between the IR spectra of random coil, α-helical, β-sheet, β′-sheet, and turn structures of polypeptides (9). These differences arise from the dependence of interactions between the various amide groups on the local polypeptide structures. One can therefore conceive of carrying out time-resolved IR capable of following the kinetics of structure change as it affects these different spatial regions of the polypeptide backbone. Experiments on the kinetics of folding also require that the system be triggered to suddenly change. For this purpose we have developed an ultrafast temperature jump (T-jump) method.

The publication costs of this article were defrayed in part by page charge payment. This article must therefore be hereby marked "*advertisement*" in accordance with 18 U.S.C. §1734 solely to indicate this fact.

The protein RNase A was chosen for the present study because of the wealth of information available regarding its equilibrium properties around the denaturation temperature and its kinetic properties on the time scale of stopped-flow experiments. The crystal structure of RNase A is known (10). The unfolding process was studied previously by static temperature methods (11–13), fluorescence (14), x-ray scattering and Fourier-transform IR (15, 16), NMR (17–20) and CD (21) spectroscopy. In denaturing, the native protein first relaxes toward an unfolded intermediate state, which then slowly equilibrates with more fully denatured structures. The fast unfolding step(s) involves the dismantling of the protein secondary structure, whereas the slower ones have been attributed to specific isomerizations involving the proline residues. "Fast" in this context has previously meant tens of milliseconds; the "very fast" intermediate reported recently (14) also has a millisecond lifetime. The time resolution of solution mixing experiments is too slow to resolve the range of protein conformational states that might occur in the earlier stages of unfolding. Molecular dynamics simulations (22–24) suggest that picosecond resolution will be needed to characterize the relevant structural changes which include significant motions along dihedral angle coordinates of the polypeptides and the modification of hydrogen-bonded structures by water (25).

To obtain a T-jump in the solution on the picosecond time scale the protein is dissolved in a solution containing inert dye molecules having a large extinction coefficient and fast internal conversion. The temperature of the solution is raised quickly by irradiating the dye transducer with an intense laser pulse. Transient IR spectroscopy is then used to measure the protein spectral response to the T-jump and also the time dependence of the temperature of the medium.

MATERIALS AND METHODS

Sample Preparation. Bovine pancreatic RNase A was obtained from Sigma (catalogue no. R-5125) and used without further purification. The solution of protein and dye buffered at p^2H (pD) 5.7 by 2-(*N*-morpholino)ethanesulfonate (Mes) was thermostatted in a temperature-controlled bath. A peristaltic pump circulated the sample from the container to the sample cell. The sample temperature was maintained at 59°C.

Transient IR Method. To monitor changes in the IR portion of the spectrum, we constructed a neodymium–yttrium/aluminum garnet (Nd–YAG) laser-based T-jump apparatus. One 35-ps pulse from an active/passive mode-locked Nd–YAG laser (1064 nm) operating at 10 Hz was selected by a KD*P Pockèls Cell (deuterated potassium dihydrogen phosphate; Medox) and amplified to 5 mJ in a three-stage Nd–YAG amplifier, then frequency-doubled in KDP (potassium dihydrogen phosphate) to produce 532-nm light of 0.6–1 mJ in energy. To generate the mid-IR at 3–5 μm, a portion of the 532-nm light was used to pump a traveling-wave dye laser whose output was mixed in $LiIO_3$ with the 532-nm pulse to produce the difference frequency. The 6-μm radiation was

Abbreviations: T-jump, temperature jump; CV, crystal violet; mOD, OD milliunits.

generated parametrically (26) from the 1.064-μm beam collimated to a 2-mm spot size in a $AgGaS_2$ crystal (41° cut). To excite the dye, the intense 532-nm pulse was focused with a 20-cm lens to a spot of diameter 300 μm. The sample cell had CaF_2 windows and a path length of 50 μm. A fresh sample was exposed with each laser shot. Both sample and reference probe beams were monitored with separate HgCdTe detectors. Not all of the experiments involve the same magnitude of T-jump, because of the different levels of discrimination used to narrow the distribution of pump pulse energies.

T-Jump Method. To induce unfolding in RNase A, we used an optically generated heat pulse to raise the temperature. Lasers have been used before to induce T-jumps in solution, normally on a nanosecond-to-microsecond time scale (27–32). In an absorbing organic medium, T-jumps of tens of degrees can be achieved within 10 ps (33) by means of IR-absorbing dyes with picosecond relaxation times and almost unit efficiency for internal conversion. In extending this approach to protein solutions we have sought water-soluble dye transducers, one example of which is the triphenylmethane dye crystal violet (CV). CV has very efficient internal conversion (34–36) that leads to rapid heating of its environment.† It is crucial for the interpretation of the heating dynamics that the protein and dye are independently and homogeneously dispersed in the solution.

The T-jump technique was quantitatively analyzed by studies in the absence of protein. When CV was dissolved in aqueous solution (1.5 mM, 9×10^{17} molecules per cm^3) and pumped by the 532-nm pulse, a reduction in absorbance signal at 2270 cm^{-1} due to the heating of the bulk water (H_2O in this example) within the beam volume (≈1 nl) was observed. The change in water absorption shown in Fig. 1 rises within the period of the instrument function of 45 ps and becomes constant thereafter. The temperature rise in this experiment is 10 ± 1 K. As discussed below this measured temperature is an average and does not represent a uniform bulk temperature until ≈70 ps after the energy deposition at the dye concentrations used in the experiment. The experiments on the solutions containing protein were carried out in the same manner, but probed also in the amide I region, 1600–1700 cm^{-1}.

The pulse energy (joules) required to raise the water temperature by 1 K is $4.2\,\nu/\alpha$, where ν is the irradiated volume and α is the fraction of incident light absorbed by the dye. In the present case $\nu = 3.5 \times 10^{-6}$ cm^3 and $\alpha = 0.18$, yielding 81.7 μJ for the required energy. Thus we expected a temperature rise of about 7 K for an ≈500-μJ incident pulse, which is close to what was measured.

Dye–Protein Interactions Are Absent. Three methods were used to establish the absence of dye-protein interaction. (*i*) Static Fourier-transform IR difference spectra were taken of the RNase A solution before and after addition of the CV over a period of 2 hr. No spectral changes of >0.9% of the overall absorbance were observed, indicating that the addition of dye caused no measurable unfolding of the protein. (*ii*) The optical transitions of the dye are known to be sensitive to changes of solvent environment (38–40), but when the UV/visible spectra of CV in water were compared in the presence and absence of the protein, the peak positions, ratios of peak heights of both the 306-nm and 540-nm bands, and widths of the bands were the same within 0.3%. (*iii*) Molecular weight resolution experiments were performed on the RNase A/dye mixture. A Sephadex G-25 gel filtration column (fractionation range, 1000–5000 Da) was prepared in Mes buffer at pH 5.7. The protein/dye solution was eluted through the column. Complete recovery of protein occurred within the first 25 ml of eluate, with no measurable coelution of dye. There was no evidence for any dye–protein association in any of these experiments. Therefore, in what follows we assume that CV and protein are independently dispersed in the solution.

†Another approach is to use as the heat transducer a protein whose cofactor undergoes rapid internal conversion. One example is myoglobin: after optical excitation the heme rapidly cools resulting in a jump, within ≈10 ps, of the surrounding water temperature (see ref. 37). We have demonstrated that this approach is also viable for T-jump experiments, although at very high excitation fluences unwanted photochemical reactions and shock waves were observed.

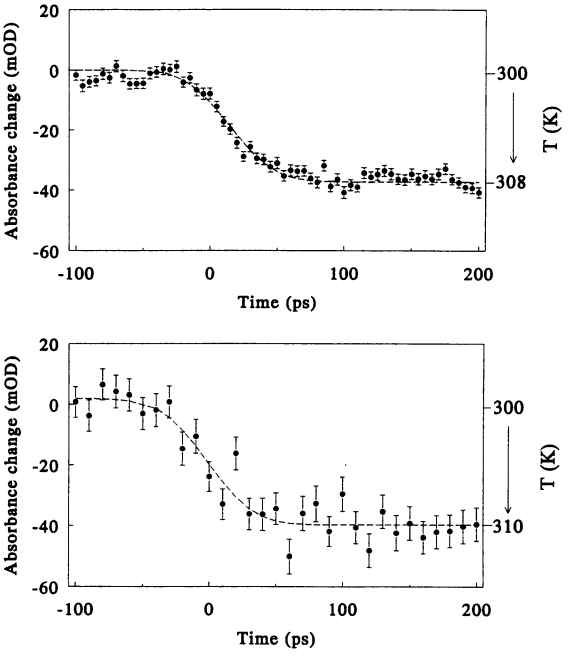

FIG. 1. Time dependence of the change in IR absorption of H_2O at 2270 cm^{-1} resulting from 1064-nm pumping of Cyasorb IR-165 dye (1.5 mM in 0.5% sodium dodecyl sulfate) (*Upper*) or 532-nm pumping of crystal violet (1.5 mM in pH 5.7 solution) (*Lower*). The right-hand ordinate corresponds to the average temperature as defined in the text. mOD, OD milliunits.

RESULTS AND DISCUSSION

Time Scale of the T-Jump of the Protein. The time resolution of this T-jump method is set by three controllable factors: the width of the excitation pulse, the relaxation times of the dye and response of the solvent to heating, and the time delay in obtaining a uniformly heated solution.

Previous work with the related dye malachite green, which, after excitation, also undergoes rapid internal conversion to create highly excited (hot) ground-state molecules (35, 37, 41–46), showed that the full temperature increase of the water was attained 4 ps *after* the energy deposition process (37). These transient events occur rapidly compared with the time scale of the experiments reported here and can be neglected. Of greater importance is the temperature variation of the water IR spectrum. The absorption coefficient of water at the frequencies used and over the temperature ranges employed in this experiment is essentially linear with temperature (37, 46–50). It follows that optical-density changes in the IR spectrum of the heated water should be independent of the spatial distribution of deposited energy or temperature. That is, the absorbance change of water is not sensitive to the dynamics of the thermal diffusion from the hot spots created by the cooling dye molecules. Thus the water temperature quoted in the subsequent parts of this paper is necessarily an "average temperature" $T(t)$. The time dependence concerns only the rate of energy deposition and water response. At times long compared with that for thermal energy to diffuse over the

distance separating dye molecules, the system is heated homogeneously and the bulk temperature will equal T ($t > 4$ ps).

The laser pulse width of ≈25 ps is considerably greater than the relaxation time of the dye (<1 ps) and the spectral response time for impulsively heated water [≈4 ps (37)]. After the laser pulse is absorbed, the sample has not necessarily reached an equilibrium temperature. At the concentrations of dye (9×10^{17} molecules per cm^3) and protein (4.5×10^{17} molecules per cm^3) used in the experiments, the mean nearest-neighbor distance‡ between any pair of solutes is 50 Å and that between dye molecules is 57 Å. The spatial distribution of heat energy released by each dye molecule should be predictable by classical heat diffusion for times larger than a few tens of picoseconds, so that $\exp[-r^2/4\chi t]$ is the ratio of the energy (temperature) found at distance r from the dye to that at the origin (the dye location) after time t (52). Thus the time at which this distribution will achieve a variance of (50 Å)^2 is obtained from $(2\chi t)^{1/2} = 5.0 \times 10^{-7}$ cm, which yields $t = 113$ ps, where χ is the water thermal diffusion coefficient of 1.11×10^{-3} cm^2 sec^{-1}. It follows that there is a waiting time until the profile of the heat released by the dye will be contained in a volume large enough to incorporate a protein. If required, the time resolution could be improved by increasing the protein concentration.

A proper assessment of the time resolution of the protein heating experiment requires that all the dye molecule heat sources be considered. An infinite lattice model for the spatial distribution of excited dye molecules in the solution yields an approximation to the bulk medium. With the protein at the origin and dye molecules located at all lattice points on a cubic lattice with cell dimension d, the temperature at the origin is obtained by summing the contributions at each time t from each point heat source at r_i. The result, which uses the well-known formula for heat diffusion from a point source (52), is readily seen to be given by

$$T_{\text{total}}(t) = \Sigma\, T_i(r_i, t) = \frac{q}{8(\pi\chi t)^{3/2}} \sum_i e^{-r_i^2/4\chi t}$$

$$= \frac{q}{8(\pi\chi t)^{3/2}} \left\{ \left[2 \sum_{l=0}^{\infty} e^{-Bl^2} - 1 \right]^3 - 1 \right\},$$

where $B = d^2/4\chi t$, q is the strength (52) of each source, and l is an integer. The limit of the sum over all dye molecules in the irradiated volume was taken to be infinity without loss of accuracy. A plot of this function is shown in Fig. 2 for the conditions of the experiments reported here. The lattice spacing, d, was chosen to be the mean value of the nearest-neighbor distribution. This temperature is seen to rise with a time constant of 50 ps and does not change with time beyond ≈100 ps. Thus we may safely conclude that the protein and its immediate environment have fully reached the new temperature by 70 ps after the T-jump impulse under the present experimental conditions. We adopt this as the time resolution of the T-jump. These same considerations would apply if the water vibrations were directly excited by the laser pulse.

Change in the IR Spectrum of the Protein Amide I Region. The first experiment probing the amide I (C=O stretching) region of RNase A measured the time dependence of the C=O absorption in a spectral region that is associated with β-sheet structures (1630 cm^{-1}) following a T-jump from 59°C to 62.5°C. The bleaching signal arising from depletion of β-sheet C=O was the largest overall signal in the static temperature-difference IR spectra (15, 16). The raw time-dependent signal

‡The mean nearest-neighbor separation between randomly dispersed particles at number density n is given by the equation $4\pi n \int_0^\infty \exp[-4\pi n r^3/3] r^3 dr = 0.554/n^{1/3}$ (see, for example, ref. 51).

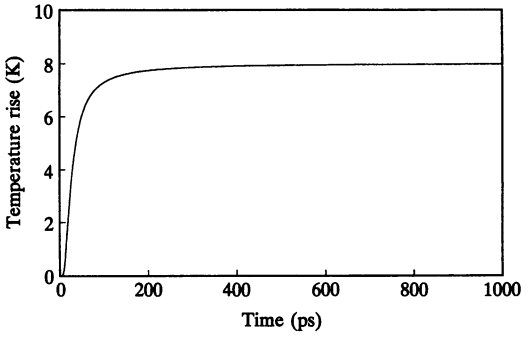

FIG. 2. Calculation of the time dependence of the temperature at the center of a protein arising from an infinite array of point heat transducers. Dye (CV) concentration was 9×10^{17} molecules per cm^3.

from the protein solution (Fig. 3 *Upper*) exhibits an initial change due to the change in D_2O absorbance with temperature that is discussed above. In addition to this background signal there is a further bleach that is present only when there is protein in the solution. Furthermore, this signal is absent if, prior to the T-jump, the solution is more than 10°C below the denaturation temperature. The amide I regions near 1666 cm^{-1}—which are anticipated to be associated mainly with random coils, bends, α-helix and turns—exhibit similar kinetic signals except that the slow component beyond 1 ns is an increasing absorption signal, consistent with expectations from the equilibrium difference IR spectra. This is unequivocal evidence that these slower signals are due to changes in the IR spectra of the protein. The raw kinetic data were adjusted to remove the pure solvent contribution, which is accurately known as demonstrated by the examples in Fig. 2, and the corrected signals are shown in Fig. 3 *Lower*. The data are not

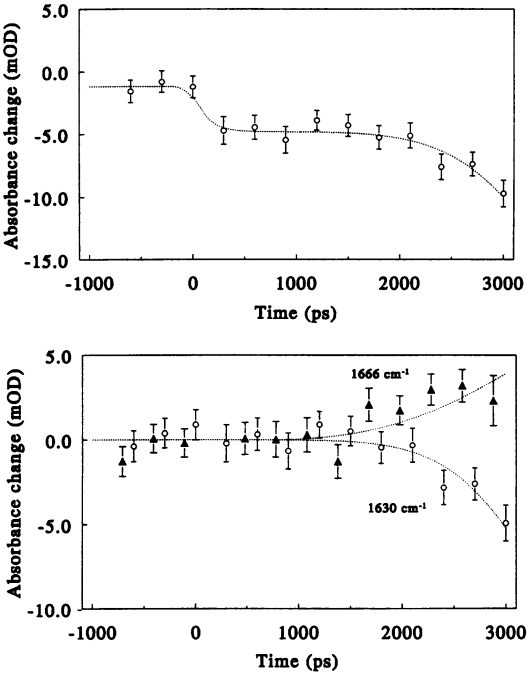

FIG. 3. Time dependence of the absorbance change in the amide I region of RNase A/D_2O following a T-jump at $t = 0$. (*Upper*) Raw data for response at 1630 cm^{-1} for a T-jump of 3.5 K (59°C to 62.5°C), including the D_2O background response. (*Lower*) Background-corrected data for 1666 cm^{-1} (▲; T-jump from 59°C to 65°C) and 1630 cm^{-1} (○; T-jump from 59°C to 62.5°C). Dotted line is a compressed exponential fit to $+9.2\,\{1 - \exp[-(t/3.8)^4]\}$ (for 1666 cm^{-1}) or $-17.1\,\{1 - \exp[-(t/3.55)^6]\}$ (for 1630 cm^{-1}).

good enough to prove that there is a significant difference in the kinetics of the 1666-cm^{-1} absorption increase and the 1630-cm^{-1} absorption decrease, but the indication of this is evident (Fig. 3 *Lower*).

In another experiment, a delay of 3.5 ns was maintained between T-jump and probe pulses and the IR probe was tuned to selected wavelengths between 1600 and 1700 cm^{-1} in order to generate the spectrum of the unfolding protein. The data as shown in Fig. 4 were corrected for the known D_2O background response. Included in Fig. 4 is the difference in the equilibrium IR spectra recorded at the same concentration used in the time-resolved experiments. The spectrum taken at 3.5 ns and the equilibrium difference spectrum, also in Fig. 4, do not show any differences that are worthy of detailed discussion given the signal/noise ratio of the experiment. Although a somewhat broader positive band is seen near 1660 cm^{-1}, further study of these differences will have to await improvements in the apparatus.

We carried out a separate experiment to determine more accurately the fractional change in absorbance at 1632 cm^{-1}: At a time delay of 5.5 ns the change in optical density was 3.7 ± 0.5 mOD for a T-jump at 60°C of 5°C. This corresponds to a 15 ± 2% change in protein absorbance.

Structural and Dynamical Features of the Ultrafast Unfolding. According to previous studies using low angle x-ray scattering and Fourier-transform IR spectroscopy (15), the thermally denatured state of RNase A is considerably more compact than expected for a Gaussian random coil and contains residual secondary structure. Between 58°C and 66°C the protein undergoes a transition from a native state that has a crystal-like radius of gyration (R_G) of 15 Å to a denatured state with R_G = 19.3 Å, whereas the R_G for a random coil exceeds 41 Å. Below 61°C the protein is folded and the (reversible) transition to the unfolded but compact state is complete at 67°C. This compact, denatured, biologically inactive form has residual secondary structure amounting to as much as 50–67% of the β-sheet found in the native forms (15, 16, 53, 54).

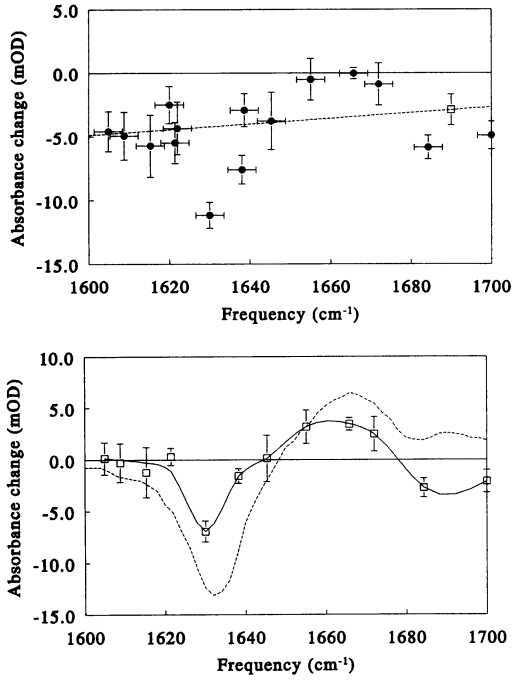

FIG. 4. Spectral response of RNase A/D_2O at 3.5 ns after a T-jump. (*Upper*) Raw data showing the absorbance difference measured; error bars indicate the uncertainty in the absorbance measurement (vertical bar) as well as the uncertainty in the IR frequency measurement (horizontal bar), determined by the bandpass of the monochromator (±3.5 cm^{-1}). Dotted line is the measured response of the D_2O for an equivalent T-jump with an error bar to indicate the uncertainty associated with this measurement (□). (*Lower*) Background-corrected spectra with raw data points within 2 cm^{-1} of each other averaged together; the solid line through the points is meant as a guide to the reader. The dashed line is the equilibrium static difference spectrum in arbitrary units.

The different portions of the IR spectra in the amide I region of RNase A have not been definitely assigned to particular polypeptide structures (15, 16). However, the region 1620–1640 cm^{-1}, specifically the band centered at 1633 cm^{-1}, is very likely a signature of β-sheet structure (15, 16). From 1640 to 1700 cm^{-1} the absorption can reasonably be assumed to consist of overlapping contributions from α-helix, turns, bends, random coils, and β-sheets.

A main feature of our results is that the intensity of the IR band associated mainly with the β-sheet region shows ultrafast changes in response to a T-jump that will ultimately convert the stable form of RNase A into the compact thermally denatured state. The difference between the spectra of the native and thermally perturbed states at 3.5 ns after the T-jump resembles closely the difference between the equilibrium states at 59°C and 65°C. This suggests that 15% of the population of a structure having amide I absorption similar to that of the compact denatured state could be present after 5.5 ns. However, the kinetics are not characterized by a single exponential response to the T-jump: there is a significant delay of ≈1 ns before any change is detected. By 5.5 ns the change corresponds to 15% of that obtained by equilibrium measurements (15). This delay is unrelated to the dynamics of the temperature distribution. The fits to the kinetics in Fig. 3 *Lower* employ compressed exponentials only as convenient representations of the nonlinear response, whose functional form remains to be determined. (Note that different constants were needed to fit the 1630- and 1666-cm^{-1} data.) There is clearly a reduction in the β-sheet IR absorption at 1630 cm^{-1}. One interpretation of these results at 1630 cm^{-1} is that the change in intensity of the amide I absorption corresponds to a reduction in the amount of secondary structure, mainly β-sheet. Another is that the β-sheet, while remaining intact, has undergone structural alterations that modify the IR intensity in the amide I region. This partial dismantling or perturbation of the β-sheet appears to involve a cooperative response to the T-jump when observed via the IR intensity of the amide I bands. The occurrence of an induction period during which there is no detectable change in the IR absorption suggests that critical intermediate configurations need to be attained before the spectral changes can occur. These configurations must have amide I absorptions that are similar to the β-sheet, and the β-sheet structure must become unstable or significantly perturbed once a sufficient number of these configurations is achieved. We cannot tell whether the observed change in the β-sheet IR absorption continues toward equilibrium as an exponential process on the nanosecond time scale. In any event it is clear that the alteration of the β-sheets involves more than one kinetic step, so that the generally accepted unfolding model for RNase A (19, 55–57), in which a so-called fast unfolding kinetic component (U_f) is reached in a single kinetic step, does not predict our results. The kinetics we observe are quite different from those reported in chemical mixing experiments that used tyrosine absorption as a probe (14). In that work the first changes detected were on the millisecond timescale. However, as noted in ref. 14, the time change in the environment of an aromatic chromophore is not a direct measure of all the actual events of unfolding. We can say that significant changes are occurring 6 orders of magnitude in time sooner than the changes detected in the chemical mixing experiments.

It is unlikely that major changes in the dispositions of sheets, helices, bends, and turns could have occurred within the 1-ns time interval prior to the observed changes. The protein undergoes a total increase in R_G of only ≈29% on denaturation

(15). In order to break up the β-sheet structure it is clearly advantageous that hydrogen bonds be formed with the β-strands, and water should be ideal for this purpose. Thus one structural interpretation of the critical configurations is that they arise from water molecules that seep into the normally hydrophobic β-sheet region as a result of small structural changes and expansion of the protein induced by the T-jump, and that these water molecules reach regions that facilitate breaking the hydrogen bonds of the β-sheet when appropriate local distortions occur. Water molecules might alter the amide I absorption without totally disrupting the β-sheets. Heat capacity measurements have indicated that in the unfolded state of RNase A there is significant hydration of naturally hydrophobic groups (58). The importance of water to the early stages of protein unfolding was proposed recently as a result of molecular dynamics simulations on the protein barnase (25). This theoretical work demonstrates that at high temperatures water molecules can diffuse into hydrophobic regions of barnase (which, unlike RNase A, does not have disulfide bonds) and dismantle the β-sheet on a time scale of ≈70 ps. This is considerably faster than the 1-ns delay observed in this work with RNase A. With improvements in the frequency range and signal/noise ratio of the technique introduced here, it should be possible to investigate such intermediate hydrogen-bonded states directly.

We are greatly indebted to Professor Walter Englander for his helpful comments on this research and Professor Ponzy Lu for valuable suggestions regarding dye/protein binding. This research was supported by the National Institutes of Health and the National Science Foundation and by the Laser Facility at the University of Pennsylvania (a National Institutes of Health Regional Resource).

1. Englander, S. W. & Mayne, L. (1992) *Annu. Rev. Biophys. Biomol. Struct.* **21,** 243–265.
2. Kim, P. S. & Baldwin, R. L. (1990) *Annu. Rev. Biochem.* **59,** 631–660.
3. Sali, A., Shakhnovich, E. & Karplus, M. (1994) *Nature (London)* **369,** 248–251.
4. Skolnick, J., Kolinski, A. & Godzik, A. (1993) *Proc. Natl. Acad. Sci. USA* **90,** 2099–2100.
5. Jones, C. M., Henry, E. R., Hu, Y., Chan, C. K., Luck, S., Bhuyan, A., Roder, H., Hofrichter, J. & Eaton, W. A. (1993) *Proc. Natl. Acad. Sci. USA* **90,** 11860–11864.
6. Anfinrud, P. A., Han, C. & Hochstrasser, R. M. (1989) *Proc. Natl. Acad. Sci. USA* **86,** 8387–8391.
7. Locke, B., Diller, R. & Hochstrasser, R. M. (1993) in *Biomolecular Spectroscopy*, eds. Clark, R. J. H. & Hester, R. E. (Wiley, New York), Part B, Vol. 20, pp. 1–43.
8. Hochstrasser, R. M. (1995) in *Monographs on Chemistry in the 21st Century Series, International Union of Pure and Applied Chemistry,* ed. El-Sayed, M. A. (Blackwell, Boston), in press.
9. Krimm, S. & Bandekar, J. (1986) *Adv. Protein Chem.* **38,** 181–364.
10. Borkakoti, N., Moss, D. S. & Palmer, R. A. (1982) *Acta Crystallogr. B* **38,** 2210–2217.
11. Chen, M. C. & Lord, R. C. (1976) *Biochemistry* **15,** 1889–1897.
12. Lustig, B. & Fink, A. L. (1992) *Biochim. Biophys. Acta* **1119,** 205–210.
13. Fink, A. L. & Painter, B. (1987) *Biochemistry* **26,** 1665–1617.
14. Houry, W. A., Rothwarf, D. M. & Scheraga, H. A. (1994) *Biochemistry* **33,** 2516–2530.
15. Sosnick, T. R. & Trewhella, J. (1992) *Biochemistry* **31,** 8329–8335.
16. Seshadri, S., Oberg, K. A. & Fink, A. L. (1994) *Biochemistry* **33,** 1351–1355.
17. Udgaonkar, J. B. & Baldwin, R. L. (1988) *Nature (London)* **335,** 694–699.
18. Mayo, S. L. & Baldwin, R. L. (1993) *Science* **262,** 873–876.
19. Udgaonkar, J. B. & Baldwin, R. L. (1990) *Proc. Natl. Acad. Sci. USA* **87,** 8197–8201.
20. Akasaka, K., Naito, A. & Nakatani, H. (1991) *J. Biomol. Nucl. Magn. Res.* **1,** 65–70.
21. Scholtz, J. M. & Baldwin, R. L. (1993) *Biochemistry* **32,** 4604–4608.
22. Soman, K. V., Karimi, A. & Case, D. A. (1993) *Biopolymers* **33,** 1567–1580.
23. Tirado-Rives, J. & Jorgensen, W. L. (1991) *Biochemistry* **30,** 3864–3871.
24. Loncharich, R. J. & Brooks, B. R. (1990) *J. Mol. Biol.* **215,** 439–455.
25. Caflisch, A. & Karplus, M. (1994) *Proc. Natl. Acad. Sci. USA* **91,** 1746–1750.
26. Elsaesser, T., Seilmeier, A., Kaiser, W., Koidl, P. & Brandt, G. (1984) *Appl. Phys. Lett.* **44,** 383–385.
27. Hoffmann, H., Yeager, E. & Stuehr, J. (1968) *Rev. Sci. Instrum.* **39,** 649–653.
28. Beitz, J. V., Flynn, G. W., Turner, D. H. & Sutin, N. (1970) *J. Am. Chem. Soc.* **92,** 4130–4132.
29. Turner, D. H., Flynn, G. W., Sutin, N. & Beitz, J. V. (1972) *J. Am. Chem. Soc.* **94,** 1554–1559.
30. Holzwarth, J. F. (1979) in *Techniques and Applications of Fast Reactions in Solution*, eds. Gettins, W. J. & Wyn-Jones, E. (Reidel, Berlin), pp. 47–70.
31. Ameen, S. (1975) *Rev. Sci. Instrum.* **46,** 1209–1215.
32. Smith, J. J., McCray, J. A., Hibbard, M. G. & Goldman, Y. E. (1989) *Rev. Sci. Instrum.* **60,** 231–236.
33. Chen, S., Lee, I.-Y. S., Tolbert, W. A., Wen, X. & Dlott, D. D. (1992) *J. Phys. Chem.* **96,** 7178–7186.
34. Magde, D. & Windsor, M. W. (1974) *Chem. Phys. Lett.* **24,** 144–148.
35. Ben-Amotz, D. & Harris, C. B. (1987) *J. Chem. Phys.* **86,** 4856–4870.
36. Sundstrom, V., Gillbro, T. & Bergstrom, H. (1982) *Chem. Phys.* **73,** 439–458.
37. Lian, T., Locke, B., Kholodenko, Y. & Hochstrasser, R. M. (1994) *J. Phys. Chem.* **98,** 11648–11656.
38. Lewis, G. N., Magel, T. T. & Lipkin, D. (1942) *J. Am. Chem. Soc.* **64,** 1774–1782.
39. Schiller, R. L., Coates, J. H. & Lincoln, S. F. (1984) *J. Chem. Soc. Faraday Trans.* **80,** 1257–1266.
40. Valiente, M. & Rodenas, E. (1991) *J. Phys. Chem.* **95,** 3368–3370.
41. Ippen, E. P., Shank, C. V. & Bergman, A. (1976) *Chem. Phys. Lett.* **38,** 611–614.
42. Mokharti, A., Chebira, A. & Chesnoy, J. (1990) *J. Opt. Soc. Am. B* **7,** 1551–1557.
43. Mokhatari, A., Fini, L. & Chesnoy, J. (1987) *J. Chem. Phys.* **87,** 3429–3435.
44. Migus, A., Antonetti, A., Etchepare, J., Hulin, D. & Orszag, A. (1985) *J. Opt. Soc. Am. B* **2,** 584–594.
45. Robl, T. & Seilmeier, A. (1988) *Chem. Phys. Lett.* **147,** 544–550.
46. Draegert, D. A., Stone, N. W. B., Curnutte, B. & Williams, D. (1966) *J. Opt. Soc. Am.* **56,** 64–69.
47. Ganz, E. (1937) *Ann. Phys.* **28,** 445–457.
48. Fox, J. J. & Martin, A. E. (1940) *Proc. R. Soc. London A* **174,** 234–262.
49. Hartman, K. A., Jr. (1966) *J. Phys. Chem.* **70,** 270–276.
50. Senior, W. A. & Verral, R. E. (1969) *J. Phys. Chem.* **73,** 4242–4249.
51. Chandrasekhar, S. (1943) *Rev. Mod. Phys.* **15,** 1–89.
52. Carslaw, H. S. & Jaeger, J. C. (1959) *Conduction of Heat in Solids* (Clarendon, Oxford), pp. 192–195.
53. Robertson, A. D. & Baldwin, R. L. (1991) *Biochemistry* **30,** 9907–9914.
54. Johnson, W. C. (1988) *Annu. Rev. Biophys. Biophys. Chem.* **17,** 145–166.
55. Nall, B. T., Garel, J. R. & Baldwin, R. L. (1978) *J. Mol. Biol.* **118,** 317–330.
56. Schmid, F. X. & Baldwin, R. L. (1979) *J. Mol. Biol.* **133,** 285–287.
57. Schmid, F. X. (1983) *Biochemistry* **22,** 4690–4696.
58. Privalov, P. L., Tiktopoulo, E. I., Venyaminov, S. Y., Griko, Y. V., Maghatadze, G. I. & Khechinashvili, N. N. (1989) *J. Mol. Biol.* **205,** 737–750.